Multiscale investigation of the fate of silver during printed paper electronics recycling

Bahareh Zareeipolgardani, Agnès Piednoir, Blandine Joyard-Pitiot, Gael Depres, Laurent Charlet, Jean Colombani

Multiscale investigation of the fate of silver during printed paper electronics recycling

Bahareh Zareeipolgardani[a] , Agnès Piednoir[b], Blandine Joyard-Pitiot[c], Gael Depres[c], Laurent Charlet[a] and Jean Colombani[b]

[a]Institut des Sciences de la Terre, Université Grenoble–Alpes, CNRS, 38000 Grenoble, France; [b]Institut Lumière Matière, Université de Lyon, Université Claude Bernard Lyon 1, CNRS UMR 5306, campus de la Doua, 69622 Villeurbanne, France; [c]Arjowiggins France, 10, rue Jean Arnaud, 38500 Voiron, France

ARTICLE HISTORY

Compiled September 16, 2022

ABSTRACT

The use of printed paper electronics in consumer goods is expected to experience a mass development in the next future. The ink used in these devices contains silver nanomaterials that may be released in the environment at the product end-of-life. We report here the first evaluation of the fate of silver during a pilot-scale recycling of printed paper electronics, made of paper printed with a cellulose nanofibrils-silver nanowire ink. We show that the released effluents are mainly free from silver, which is retained in the pulp conserved for recycling. We use atomic force microscopy experiments to show that this strong pulp-silver bond is due to the embedding of the silver nanowires in the pulp by coils of cellulose nanofibrils. We propose an estimate of the resulting adhesion stress of the nanowires to the ink, high enough to keep the silver inside the pulp during the recycling procedure.

KEYWORDS

printed paper electronics, cellulose nanofibers, silver nanowire, adhesion, recycling

Corresponding author, jean.colombani@univ-lyon1.fr

1. Introduction

Electronics currently experiences a sustained evolution in various directions: The constant race toward miniaturization is progressively reaching the nanoscale; optoelectronics is developing with the spreading of mobile displays; lighter, cheaper and safer substrates are required in a growing number of applications. In this context, printed electronics fulfills several of these requirements and is expected to exhibit an exponential growth in the coming years [1].

The elaboration of electronic components by conventional printing methods on light-weight, bendable, cheap, and even wearable substrates, makes possible the embedding of organic light emitting diode, solar cells, antennas, transistors or even sensors in a large variety of structures [2]. During the fabrication, a conductive ink is printed on a low-cost substrate such as glass, paper, fabric or silk, potentially transparent [3–7]. In the three last cases, functional flexible structures may therefore be obtained at large-scale, after a relatively fast industrialization step [8,9].

Paper is one of the most common, and the cheapest, substrates hosting printed electronics. Compared to standard electronic circuit board, its incomparable advantages —it can be folded and unfolded, it is inexpensive, its weight is low, it is breathable and easily decomposes— have led to use printed paper as identification tag for mass market goods, anti-counterfeit label, shock-detection tag, purchase ticket, drug delivery or clinical diagnosis [10,11].

This extension of the range of applications of printed paper electronics was initially inspired by electronics printed on soft polymer [12], but it progressively expands by proposing devices foldable and reusable to an unprecedented extent, using sometimes aluminum ink [13,14], but more commonly silver nanoparticles [15] or silver nanowires [16,17] inks.

But the expected mass development of this printed paper electronics still faces a major challenge before its implementation. After use, the fate of the metallic, conductive, component of the material in the environment is a crucial issue, and almost nothing is known yet about it. The risk of escape of metal during the disposal or recycling of printed paper will be a central point in the integration of this technology in

consumer electronics, and even more in packaging or clothing [18]. Silver nanoparticles for example, one of the main conductive components of the inks, are known to have a possible biocidal action [19]. This toxicity is partly a consequence of their nanometer scale. Indeed, the small scale for example allows upon inhalation a preferential deposition in the deep alveolar region of the lung [20]. Moreover, it can also foster the transformation of the particles into more toxic forms of silver [21]. In this context, a determination of the long-term fate of the conductive component of the ink is a necessary step prior to the dissemination of printed paper electronics, in order to establish whether a massive release of possibly toxic metallic nanoparticles is to be feared.

In order to assess the printed paper electronics end-of-life risk, we present here the first experimental study of the fate of the silver of a commercial paper, on which a conductive ink is printed, during recycling. In this study, the choice of the ink is a crucial point and should contribute to decrease the silver release rate from the material at all stages of the paper life. We have chosen an ink made of silver nanowires (AgNW) dispersed in cellulose nanofibrils (CNF). Regarding the conductive part, whereas silver nanoparticles used in classical conductive inks are poorly crystalline, soluble and highly mobile [8], particularly in aqueous environment, making them hazardous, silver nanowires, in a fibrous shape, are highly crystalline and expected to be less mobile. Regarding the filler, nanocellulose (cellulose nanocrystals and nanofibrils) has drawn attention recently because of its striking and highly versatile particle binding ability [22]. In the particular case of conductive ink, it provides an improved adhesion to the substrate and a lower roughness [23]. It is also a better dispersing [24] and thickening [25] agent compared to standard cellulose fibers, thereby contributing to decrease the silver content of the ink.

Here, applying a standard recycling process to this printed paper, we show that its metallic component remains trapped inside the cellulose, even after a screening or a deinking procedure. The bond between the silver nanowires and the cellulose is strong enough to prevent their escape from the material even after dilution, filtering or addition of detergent. We also give an explanation for the stability of the material during this treatment based on atomic-scale experiments, investigating the attachment strength of the metallic nanowires to the cellulose substrate. We show that the

embedding of the silver nanowires by the cellulose nanofibrils, reminiscent of other coiling geometry of natural and artificial nanofibers [26], prevents from the escape of the metal in the environment, and we provide a first estimate of the detachment stress of the AgNW from the ink.

2. Materials and methods

2.1. Materials and chemicals

In order for the ink to keep its conductive nature, it is imperative that it stays at the surface of the paper. A spreading of the ink metallic component inside the substrate generally leads to the loss of its conductive behavior. For that reason, specific papers have to be used in printed paper electronics. The impermeability of these materials, impeding the ink penetration, is obtained by a lower surface porosity and higher smoothness compare to standard paper.

As explained in the introductory part, we have chosen silver nanowires as conductive component of the ink. Beside their probable less hazardous nature, these nanowires have also the particularity, due to the looser nature of the network they form compared to nanoparticles, to be quasi transparent, unlike black standard conductive ink. In order to profit from this characteristics, we have chosen as working substrate a Sylvicta paper, manufactured by Arjowiggins, composed of cellulose fibers coated by 3 μm of polyvinylidene chloride, which exhibits the transparency of a tracing paper. It is printed with PolyBioWire ink, from Poly-Ink, made of silver nanowires (AgNW), covered by a few nm of polyvinylpyrrolidone to prevent sulfidation and oxidation [27], with a 100 nm average diameter and a 5 to 15 μm length, dispersed in an aqueous suspension of cellulose nanofibrils (CNF), exhibiting a diameter from 2 to 50 nm and a length from 0.5 to 2 μm.

The 52 g/m^2 area density paper is printed with 24 g/m^2 of ink and dried at 120°C. The ink contains 0.5 % of AgNW and 0.5 % of CNF, leading to a silver area density after evaporation of the solvent of 0.12 g/m^2, corresponding to 0.2 % of silver in the ready-to-use printed paper.

2.2. Recycling process

In paper electronic devices, the printing process efficiency rests upon the permanent bond created between the conductor and its supporting substrate. Our objective here is to assess the long-term fate of this conductor, possibly harmful for health, in order to establish whether the bond survives a recycling process. For that, we have submitted a printed paper to pilot-scale recycling procedures inspired by industrial processes. Whereas the recycling of soft electronics printed on polymer requires organic solvents, we can mention that these processes only make use of water and detergent [28].

Two recycling processes, each composed of two steps, have been tested. In both cases, the first step is a *pulping* stage, aimed at separating the cellulose fibers from each other and from the silver nanowires following the ISO 5263-1 standard, in which 104 g of printed paper is stirred in 8 L of water during 15 min at a 3000 rpm rate in a so-called pulper. Afterward, for the first process, a *screening* stage, intended to remove possible contaminants of size larger than the slots, is carried out, where 2 L of the slurry resulting from the pulping stage is diluted with 7 L of water and sieved with a Somerville equipment following the T 275 SO-12 standard [29]. The filter of our sieve is a plate drilled with 45 mm long and 0.15 mm wide slots. For the second process, a *deinking* stage, aimed at separating the hydrophobic components (ink) from the hydrophilic components (fibers) [30], is performed, in which calcium chloride and surfactants are added to the 8 L of pulp, completed with water to 15 L, and bubbled with compressed air in a flotation cell during 10 min. The soap fatty acid long-chains bind both to the ink and to the bubbles and the resulting foam is collected at the surface and evacuated by overflow [31].

2.3. Chemical analyses

Induced coupled plasma optical emission spectrometry (ICP-OES) measurements of the Ag content were performed on the pulp collected at the end of each step of the procedure after sedimentation and vacuum filtration through a 0.22 μm nitrocellulose membrane. In order to measure reliably the Ag content in this waste water material, the solution sample at each step was treated so as to remove the polymer coating from

the AgNWs, which could hinder the ICP-OES measurement. This was done in three steps, inspired by protocols used in the paper industry: addition to the solution of (i) enzymes, then (ii) hydrogen peroxide (at a 30% concentration), then (iii) nitric acid (at a 65% concentration). Two calibration curves were obtained with standards made with H_2O_2 and HNO_3 at the final added concentrations (1% and 10.5%, respectively): one for 0 to 1 ppm of Ag and one for 0.5 to 23 ppm of Ag. Furthermore, all ICP measurements were performed at a fixed duration after sample preparation, namely 1 h, to avoid a differential aging effect.

2.4. Microscopic scale measurements

The characterization and manipulation of individual AgNWs were performed in air with an MFP-3D atomic force microscope (AFM) from Asylum Research (Oxford Instrument). For imaging the surface, the tapping mode was used. However, the substrate surface was too rough to use the AFM phase signal to get exploitable information about the mechanical property contrast between the AgNWs and CNFs. Therefore for the adhesion measurements only the normal and lateral force signal in contact mode were recorded and processed. Well-calibrated cantilevers from Nanoandmore were chosen according to the normal force applied to pull out the wires: PPP-CONTR cantilevers (stiffness constant 0.2 N/m) for the lower forces, and PPP-FMAuD cantilevers (stiffness constant 2 N/m) for the higher ones. To get quantitative measurements of the force applied by the tip to the substrate, the nominal spring constant has been measured using the thermal noise method [32].

3. Results and discussion

3.1. Aqueous phase results

Before the measurement campaign, three tests were performed to estimate the reliability of the protocol of Ag concentration determination. First the Ag content of several blank samples, made of water to which the standard enzyme, hydrogen peroxide and nitric acid quantity had been added, was measured. An average value of 0.1 mg/L Ag

concentration has been obtained, giving an estimate of the experimental precision.

Second the Ag content of a solution of pure nanowires has been measured, again following the same preparation procedure. The ICP-OES has given a Ag concentration of 51 mg/L for a solution containing 84 mg/L of Ag nanowires. This test indicates that the protocol gives the correct order of magnitude, thus proving that AgNWs are satisfactorily cleared from their polymer coating, oxidatively dissolved by enzymes, hydrogen peroxide and nitric acid, and Ag is thereby correctly quantified. The discrepancy between the expected and obtained values brings an estimate of the experimental accuracy.

Third the Ag content of the pure PolyBioWire ink, without substrate, has been measured. The ICP-OES has provided a 4.55 mg/L Ag concentration for an expected 11.6 mg/L concentration. The good agreement between these two values is a new proof that the preparation procedure frees the nanowires, even dispersed among the CNF of the liquid ink, from their protective coating and releases the Ag, with is thereby correctly quantified.

Once dilution factors are taken into account, the Ag concentration in the effluent from the initial pulp (just after pulping), the screened pulp (pulp cleared from the printed paper particles retained by the Somerville sieve) and the de-inked pulp (pulp cleared from the printed paper particles evacuated with the foam) is equal to 0.17, 0.5 and 0.61 mg/L respectively. Since the expected total Ag concentration was 26 mg/L, i.e., 0.2% of 104 g of printed paper diluted in 8 L, the vast majority of Ag is therefore seen to be absent from the waste water, and is consequently retained by the pulp. These results indicate that a strong link seems to have been created between the Ag and the cellulose inside the printed paper, a link that the recycling procedure is unable to break.

3.2. Nanoscale results

To get a first idea of the microstructure prevailing inside the pulp, which leads to this adhesion between the conductor and its substrate, the rejected pulp obtained at the end of the pulping and deinking protocol, i.e., the overflown foam, was oven-dried and observed with an AFM and a scanning electron microscope (SEM). The SEM

observation of the surface of the pulp is displayed in figure 1. It can be observed that the AgNWs accumulate regionally, aggregated here in the central zone of the figure. The striking feature is the fact that all the nanowires are stretched between their ends, buried in the cellulose. A close view of this characteristic arrangement, observed on the same final pulp by AFM, is shown in figure 2. This organization, where the AgNWs seem trapped by the CNF, still present after active stirring, dilution and bubbling of the paper, demonstrate qualitatively the strength of the cohesion inside the printed paper.

[Figure 1 about here.]

Thus the cohesion inside the ink appears to be a consequence of the nanowire-nanofibril entanglement and of their chemical interaction. To quantify this cohesion, we have studied the adhesion between CNF and AgNWs at the microscopic scale by AFM. We have chosen AFM to probe this adhesion because it has led to successful measurements of the mechanical properties of nanowires or nanofibers [33–35].

[Figure 2 about here.]

The thickness of the printed ink remains small, of the order of 200 nm. Thence the adhesion measurements carried out on the ink are likely to be influenced by the mechanical properties and roughness of the underlying matter. For that reason, we have run experiments on ink deposited on three different substrates: glass, Arjowiggins powercoat HD paper (cellulose fibers coated by 10 μm of calcium carbonate and titanium oxide) and Arjowiggins Sylvicta paper (see section Materials and chemicals), the root-mean-square roughness of which being 1, 10 and 100 nm respectively (for 100 μm^2 surface areas).

Before the mechanical tests, the surface morphology was first observed. Whatever the substrate, the dried ink exhibits always the same microstructure, with AgNWs building a loose and percolating network at the interconnected CNF network surface.

[Figure 3 about here.]

An example is shown in figure 3 for a Powercoat HD paper, recorded in tapping mode to avoid any modification of the surface by the tip. It can be immediately

observed that two types of geometrical nanowire-nanofibril interaction exist. The major part of the imaged AgNWs, that we have called embedded nanowires, are covered by woven CNF. The others, that we have called non-embedded nanowires, have their surface free from CNF and merely lie on the surface. Almost all the AgNWs that we have observed are at least partly embedded.

With this morphology in mind, we have subsequently used the AFM to measure the adhesion force of the AgNWs to the ink CNFs. To do so, in contact mode and at a fixed normal force, the slow scan is disabled and the tip completes one passage though a well-identified wire. An imaging performed immediately afterwards informs whether the nanowire is detached or not. If not, the tip is displaced a little (not to probe the same part of the wire, which may be damaged), the normal force is slightly increased and the procedure is repeated.

The nanowires are buried in the cellulose substrate at various depths, and the force needed to separate the nanowire from the ink CNFs has been seen to depend on their outcropping height h. Therefore, before each attempt to detach a AgNW, a one-dimensional profile was recorded along the line where the tip attacks the nanowire, to measure h (see figure 4c).

The evolution of the normal force necessary to break a nanowire, measured from the bending of the cantilever, with the outcropping height of this nanowire, measured from the profile, is shown in figure 5 for the three substrates for the embedded (left) and non-embedded (right) AgNWs. Three conclusions may be drawn from these curves.

[Figure 4 about here.]

First, for the embedded nanowires, two regimes are clearly observed, with a strong dependence of the force on the height for h values below ~ 25 nm, and a low dependence above. These two regimes have been seen to correspond to two different behaviors of the nanowires to the tip passage. In the low h regime, the AgNWs are not detached but abruptly buried by the tip while for high h they are detached from the ink CNFs. The low h regime shows that the conjunction of a small tip-nanowire contact area and a strong attachment to the ink by the embedding cellulose nanofibrils makes the nanowire detachment impossible. An example of the two situations (sinking and

detachment) is presented in figure 4. Consequently, as the embedded AgNWs slightly outcropping do not present any risk of escape from the material, being on the contrary more deeply sunk in the substrate by external forces, we have not considered them any further. Neither have we tried to investigate the nanowires trapped inside the bulk paper, even less liable to escape the material.

This situation never happened for non-embedded AgNWs, where the tip passage has always led, for a sufficient normal force, to their detachment. That is why no change of regime is observed in their force-height curve (figure 5 right).

Second, for embedded and non-embedded wires, as expected, the substrate has a noticeable influence on the detachment force, the rougher the substrate, the higher the detachment force. Indeed, to be able to grab the nanowire, the tip has to penetrate the floor neighboring the tip, and the rougher the substrate, the higher the force needed to catch the nanowire.

Third, for all attempts to unbind a nanowire with the AFM tip, the detachment and the failure of the wire occurred simultaneously. AgNWs simply displaced from their initial location, without fracture, have never been observed. This is a proof that the adhesion stress exceeds the strength of the nanowires.

[Figure 5 about here.]

From the recorded torsion of the cantilever, an estimate of the lateral force exerted on the tip during the detachment of the nanowires can be obtained. These lateral forces, leading to the breakdown of the substrate-nanowire bond, are much greater, of the order of tens of μN, than the normal forces, of the order of hundreds of nN, only sinking the tip in the substrate. Appreciating the applied stress $\sigma = F_t/S$ corresponding to this lateral force F_t is a very delicate task. Indeed the estimate of the tip-AgNW contact area S turns out to be tricky. As a matter of fact the geometry of this contact is quite complex, being the intersection between a pyramid (the tip) and a cylinder (the nanowire). Furthermore, the normal force induces a partial sinking of the tip inside the substrate, making the contact length inaccurate. Nevertheless, to get a first information on the order of magnitude of the cohesion between the substrate and the AgNW, we have attributed the value $S = h \times w$ to the contact area, with h the

outcropping height of the nanowire and w the width of the tip end ($w = 40$ nm).

The values of the detachment stress of the AgNWs from the substrate as a function of their outcropping height, and of the morphology (embedded or not) are displayed in figure 6. The dispersion of the results is high, which is not surprising. Indeed the imprecision on the value of the tip-wire contact area is a large source of uncertainty. Furthermore, in the case of the embedded wires, the weaving of the cellulose nanofibrils coiling around the wire may be highly different from one wire to the other.

[Figure 6 about here.]

But whatever this dispersion, there is no overlap between results of the embedded and non-embedded AgNWs, showing the unsurpassed cohesion brought to the ink by the embedding CNF. Boxes gathering all the values for each configuration have been drawn (figure 6), in order to better visualize the spread of the values in each configuration, and to evidence the absence of influence of the type of substrate on the detachment stress.

We would like to point out that this detachment stress is an empirical property, stemming from the combination of the bending strength of the AgNW, of the shear strength of the CNF-AgNW interface, and, for the embedded wires, of the tensile strength of the CNF, all acting simultaneously and interacting continuously. The variability of all these properties, due to the diameter dispersion of the wires and fibrils, to their structural defects, to their aging, etc. also contributes to the dispersion of the data.

We may also notice that this property is highly dependent on the geometrical characteristics of the nanowires. As the strong attachment is mainly a consequence of the entanglement of the AgNWs in the CNF, it is highly probable that longer nanowires would experience higher detachment stress.

We have argued above that for all the AgNWs we have investigated, the detachment of the nanowire is accompanied by its rupture, proof that the attachment bond is stronger than the mechanical strength of the silver nanowires. We have added in figure 6 the silver nanowire yield strength measured in the literature [34,36]. We see that all the measured detachment stresses lie above this yield strength, which is consistent

with our observations.

As the vast majority of the surfacing AgNWs are embedded, the parameter characterizing best the ability of the silver to escape the material is the detachment stress of the embedded nanowires, the average value of which is ~ 10 GPa. Even though this value is a first estimate, its order of magnitude is a guarantee that the probability of the nanowires to be ejected from the material, during their mainstream usage, as much as during the recycling process, is extremely low, which corroborates our macroscopic tests.

Our effluent measurements have shown that the silver contained in printed paper electronics after a standard recycling procedure, comprising pulping and screening or deinking steps, remains mainly trapped in the solid material used for the recycled paper and is almost absent from the effluent possibly released in the environment, proof of a strong link between the cellulose and the metal. Our atomic force microscopy measurements on printed paper electronics lead to a both qualitative and quantitative interpretation of this robustness of the silver-cellulose bond. On one side silver nanowires are for the main part embedded in coils of cellulose nanofibrils, preventing their escape. On the other side, the stress needed for detaching a AgNW from the substrate is of the order of GPa, above its tensile strength, guaranteeing its link to the cellulose.

This study proves that printed paper electronics can be safe for the environment by design, thanks to the intricate intertwining of the silver wires and cellulose fibers, stemming from their geometrical and chemical affinity. This conservation of the metal inside the pristine and recycled material thus avoids to dispose of the printed paper electronics by burning, for example, in which case the recovery of the metal in the flue gas of the incinerator requires complex chemical and heat treatments [37].

Further studies are now required to test the recycling of commercial products using printed paper electronics and estimate their safety in upscaled plants.

Acknowledgements

ICP-OES analyses have been performed using the geochimistry-mineralogy platform of ISTerre (OSUG-France). We thank Andrea Carboni for providing the solution of pure silver nanowires and Sarah Bureau and Simona Denti for the ICP-OES measurements.

Disclosure statement

The authors declare no competing financial interest.

Funding

This work is a contribution to the Labex Serenade (No ANR-11-LABX-0064) funded by the "Investissements d'Avenir" French Government program of the French National Research Agency (Agence Nationale de la Recherche - ANR) through the A MIDEX project (No ANR-11-IDEX-0001-02).

4. References

References

[1] Hoeng F, Denneulin A, Bras J. Use of nanocellulose in printed electronics: a review. Nanoscale. 2016;8:13131–13154.

[2] Nogi M, Karakawa M, Komoda N, et al. Transparent conductive nanofiber paper for foldable solar cells. Sci Rep. 2015;5:17254.

[3] Tao H, Hwang S, Marelli B, et al. Silk-based resorbable electronic devices for remotely controlled therapy and in vivo infection abatement. PNAS. 2014;111:17385.

[4] Jiu J, Wang J, Sugahara T, et al. The effect of light and humidity on the stability of silver nanowire transparent electrodes. RSC Adv. 2015;5:27657–27664.

[5] Du H, Wan T, Qu B, et al. Engineering silver nanowire networks: From transparent electrodes to resistive switching devices. ACS Appl Mater Interfaces. 2017;9:20762–20770.

[6] Zhang R, Engholm M. Recent progress on the fabrication and properties of silver nanowire based transparent electrodes. Nanomater. 2018;8:628.

[7] Kim D, Ko Y, Kwon G, et al. Micropatterning silver nanowire networks on cellulose nanopaper for transparent paper electronics. ACS Appl Mater Interfaces. 2018;10:38517–38525.

[8] Sung D, de la Fuente Vornbrock A, Subramanian V. Scaling and optimization of gravure-printed silver nanoparticle lines for printed electronics. IEEE Trans Compon Packag Manuf Technol. 2010;33:105–114.

[9] Matsuhisa N, Inoue D, Zalar P, et al. Printable elastic conductors by in situ formation of silver nanoparticles from silver flakes. Nat Mater. 2017;16:834.

[10] Siegel AC, Phillips ST, Dickey MD, et al. Foldable printed circuit boards on paper substrates. Adv Funct Mater. 2010;20:28–35.

[11] Glogic E, Futsch R, Thenot V, et al. Development of eco-efficient smart electronics for anticounterfeiting and shock detection based on printable inks. ACS Sustain Chem Eng. 2021;9:11691.

[12] Lee P, Lee J, Lee H, et al. Highly stretchable and highly conductive metal electrode by very long metal nanowire percolation network. Adv Mater. 2012;24:3326–3332.

[13] Lee HM, Lee HB, Jung DS, et al. Solution processed aluminum paper for flexible electronics. Langmuir. 2012;28:13127–13135.

[14] Lee HM, Choi SY, Jung A, et al. Highly conductive aluminum textile and paper for flexible and wearable electronics. Angew Chem. 2013;125:7872–7877.

[15] Sanchez-Romaguera V, Wünscher S, Turki BM, et al. Inkjet printed paper based frequency selective surfaces and skin mounted rfid tags: the interrelation between silver nanoparticle ink, paper substrate and low temperature sintering technique. J Mater Chem C. 2015; 3:2132–2140.

[16] Huang GW, Xiao HM, Fu SY. Paper-based silver-nanowire electronic circuits with outstanding electrical conductivity and extreme bending stability. Nanoscale. 2014;6:8495.

[17] Jeong S, Cho H, Han S, et al. High efficiency, transparent, reusable, and active pm2.5 filters by hierarchical ag nanowire percolation network. Nano Lett. 2017;17:4339–4346.

[18] Lehmann S, Toybou D, del Real AP, et al. Crumpling of silver nanowires by endolysosomes strongly reduces toxicity. PNAS. 2019;116:14893.

[19] Yu SJ, Yin YG, Liu JF. Silver nanoparticles in the environment. Environ Sci Processes Impacts. 2013;15:78–92.

[20] Theodorou I, Muller K, Chen S, et al. Silver nanowire particle reactivity with human monocyte-derived macrophage cells: Intracellular availability of silver governs their cyto-

toxicity. ACS Biomater Sci Eng. 2017;3:2336.

[21] del Real AP, Castillo-Michel H, Kaegi R, et al. Fate of Ag-NPs in sewage sludge after application on agricultural soils. Environ Sci Technol. 2016;50:1759–1768.

[22] Mattos BD, Tardy BL, Greca LG, et al. Nanofibrillar networks enable universal assembly of superstructured particle constructs. Sci Adv. 2020;6:eaaz7328.

[23] Hoeng F, Denneulin A, Krosnicki G, et al. Positive impact of cellulose nanofibrils on silver nanowire coatings for transparent conductive films. J Mater Chem C. 2016;4:10945–10954.

[24] Hoeng F, Bras J, Gicquel E, et al. Inkjet printing of nanocellulose–silver ink onto nanocellulose coated cardboard. RSC Adv. 2017;7:15372–15381.

[25] Hoeng F, Denneulin A, Reverdy-Bruas N, et al. Rheology of cellulose nanofibrils/silver nanowires suspension for the production of transparent and conductive electrodes by screen printing. Appl Surf Sci. 2017;394:160–168.

[26] Godinho M. When the smallest details count. Science. 2020;369:918–919.

[27] Chen Y, Pang L, Li Y, et al. Ultra-thin and highly flexible cellulose nanofiber/silver nanowire conductive paper for effective electromagnetic interference shielding. Composites Part A: Appl Sci Manuf. 2020;135:105960.

[28] Liu Y, Wang H, Zhu Y. Recycling of nanowire percolation network for sustainable soft electronics. Adv Electron Mater. 2021;7:2100588.

[29] Teschke K, Demers P. Screening of pulp (sommervile-type equipment) - TAPPI T 275. Technical Association of the Pulp and Paper Industry; 2012.

[30] Ackermann C, Göttsching L, Pakarinen H, et al. Papermaking potential of recycled fibre. In: Höke U, Schabel S, editors. Recycled fibre and deinking. (Papermaking Science and Technology; Vol. 07). Helsinki: Paperi ja Puu Oy; 2010.

[31] Fricker A, Thompson R, Manning A. Novel solutions to new problems in paper deinking. Pigment Resin Technol. 2007;36:141–152.

[32] Hutter J, Bechhoefer J. Calibration of atomic-force microscope tips. Rev Sci Instrum. 1993;64:1868.

[33] Guhados G, Wan W, Hutter JL. Measurement of the elastic modulus of single bacterial cellulose fibers using atomic force microscopy. Langmuir. 2005;21(14):6642–6646.

[34] Wu B, Heidelberg A, Boland JJ, et al. Microstructure-hardened silver nanowires. Nano Letters. 2006;6(3):468–472.

[35] Dolan GK, Cartwright B, Bonilla MR, et al. Probing adhesion between nanoscale cellulose fibres using afm lateral force spectroscopy: The effect of hemicelluloses on hydrogen

bonding. Carbohydr Polym. 2019;208:97–107.

[36] Zhu Y, Qin Q, Xu F, et al. Size effects on elasticity, yielding, and fracture of silver nanowires: In situ experiments. Phys Rev B. 2012;85:045443–045450.

[37] Wolffers M, Eggenberger U, Schlumberger S, et al. Characterization of mswi fly ashes along the flue gas cooling path and implications on heavy metal recovery through acid leaching. Waste Manage. 2021;134:231–240.

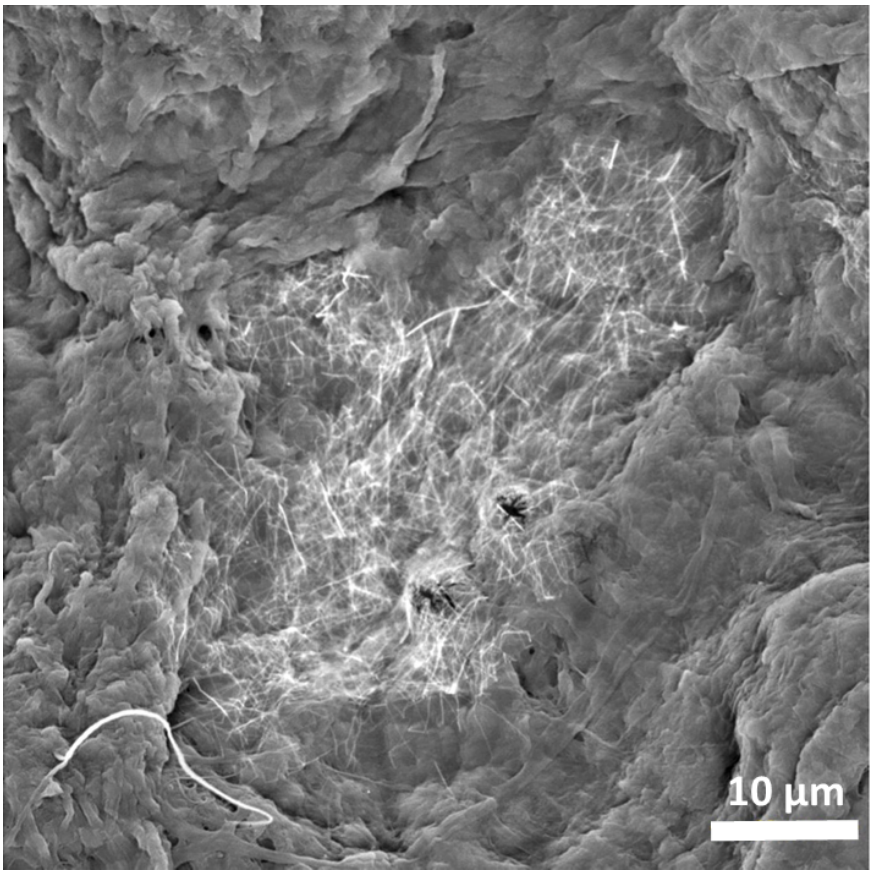

Figure 1. SEM image of the dried pulp obtained from recycled printed paper, showing accumulation of trapped AgNWs in the center (thin white straight lines).

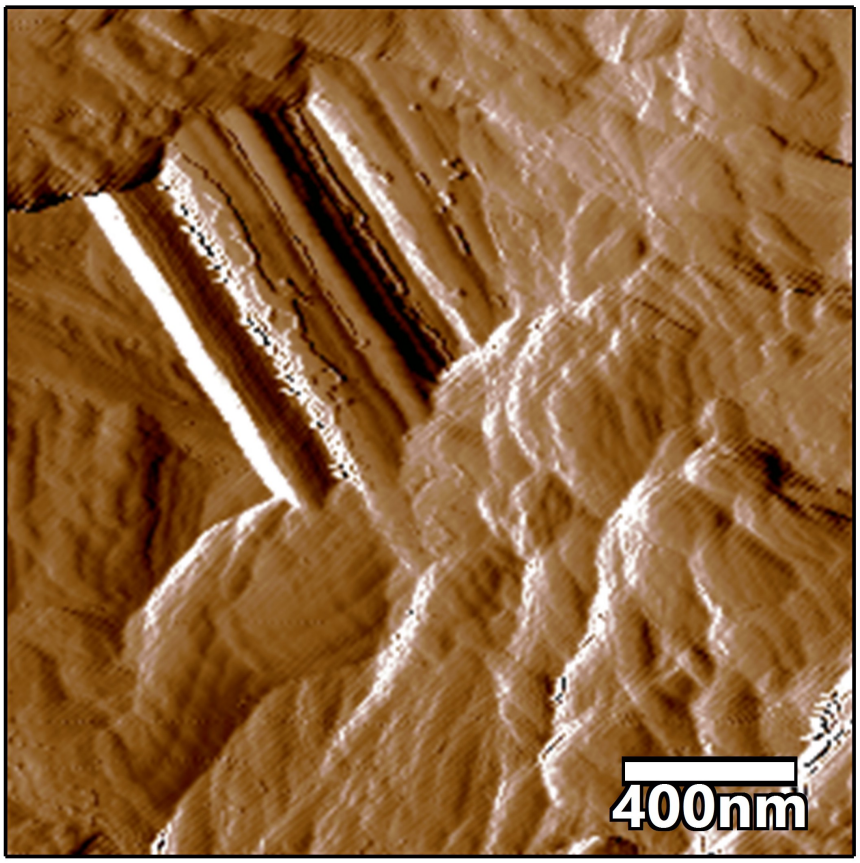

Figure 2. AFM error image of a bunch of AgNWs captured by cellulose nanofibers, in the pulp of figure 1.

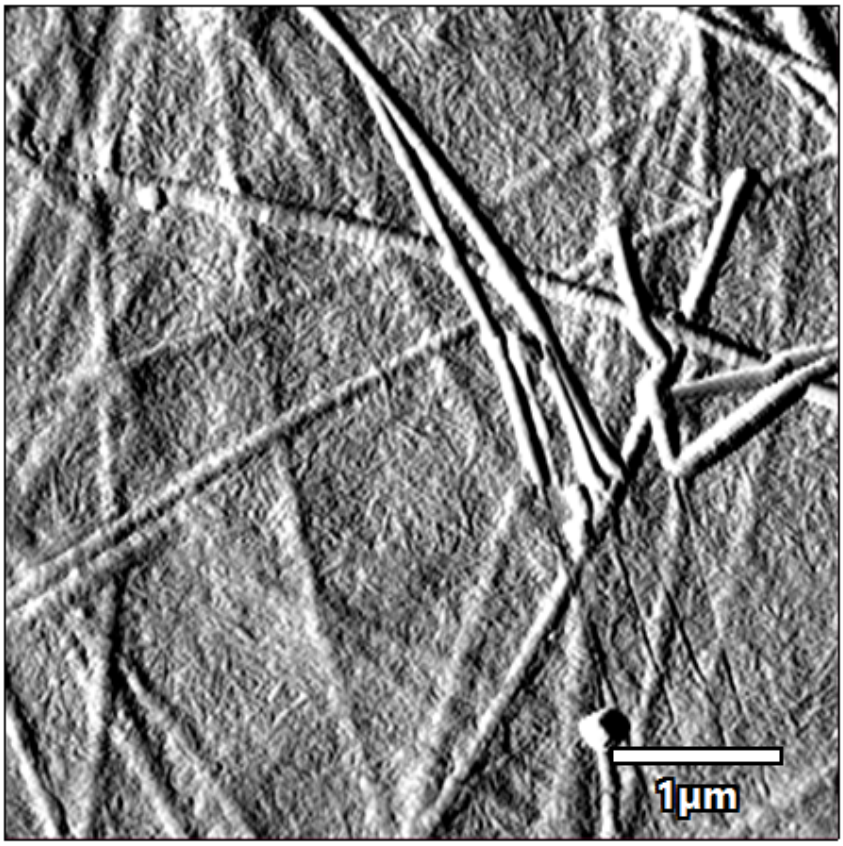

Figure 3. AFM error image of ink on powercoat HD paper. The majority of AgNWs are embedded in cellulose nanofibrils.

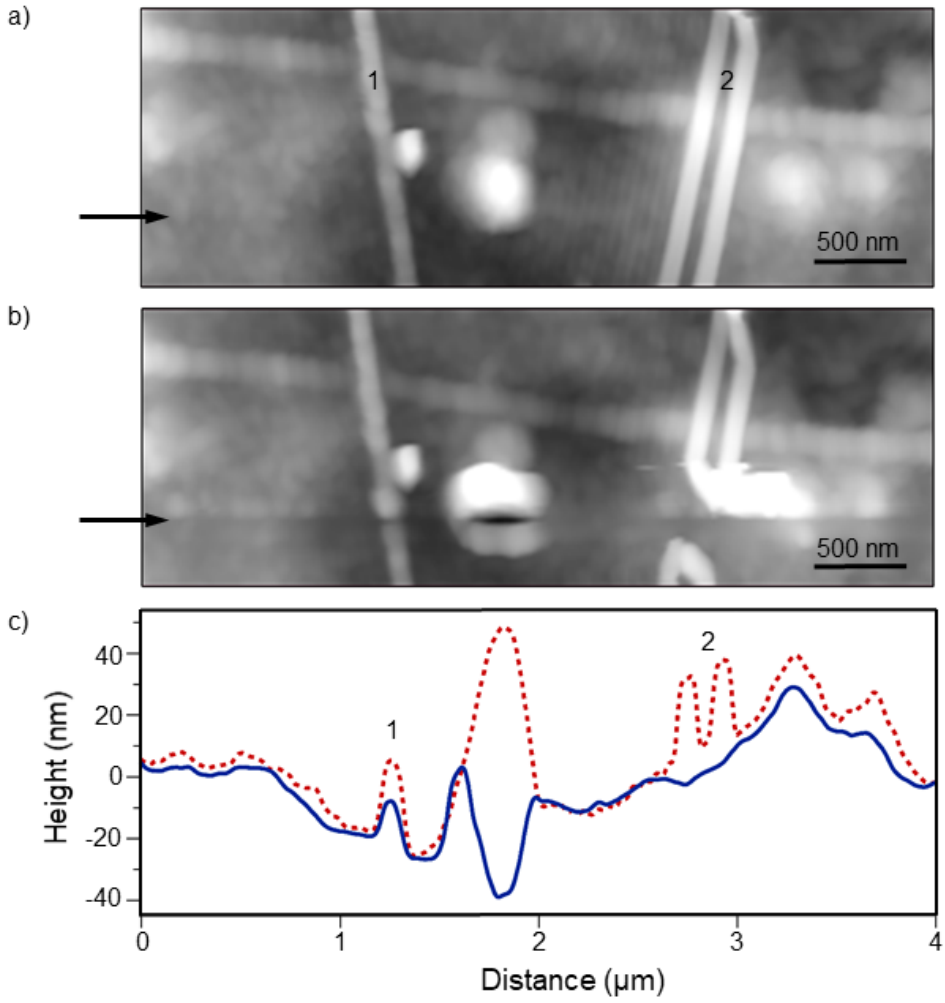

Figure 4. AFM height images (4×1.4 μm^2) of ink on Powercoat HD paper: (a) before breaking and (b) after breaking of AgNWs by the tip. (c) Profiles recorded along the scan line indicated by the black arrow, red discontinuous line before breaking and blue continuous line after breaking of the AgNWs. The embedded nanowire tagged 1 has been sunk by the tip, with an outcropping height decreased, whereas the non-embedded nanowires tagged 2 have been detached and broken, with no more outcrop.

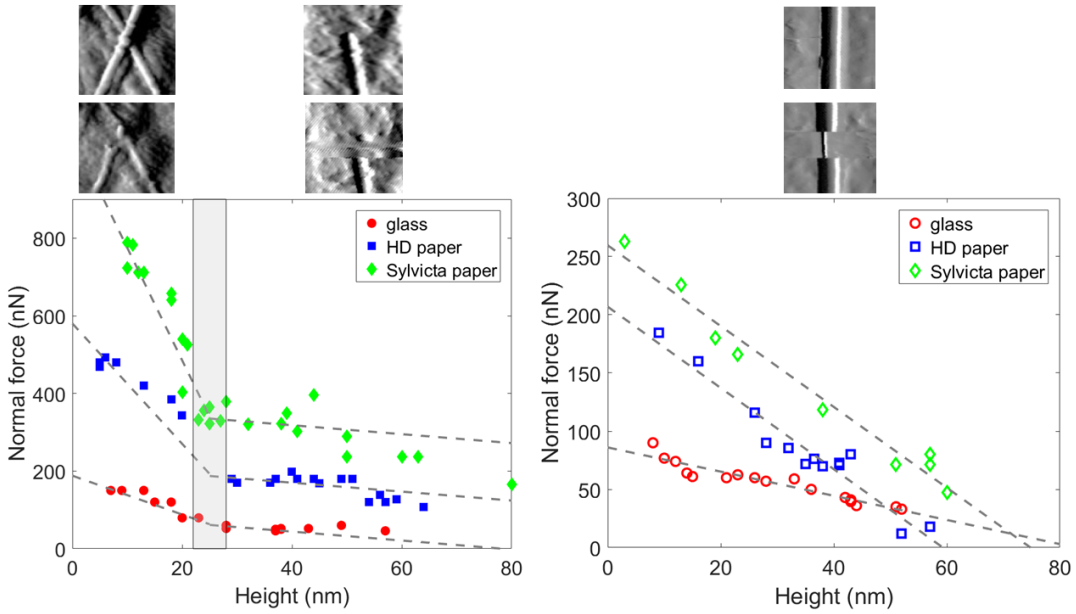

Figure 5. Normal force needed to detach or sink an embedded AgNW (left) and non-embedded AgNW (right) as a function of the outcropping height. The dashed grey lines are guides for the eye. Example (AFM error image) of nanowires before (top) and after (bottom) detachment or sinking by the tip are displayed for the 3 congurations.

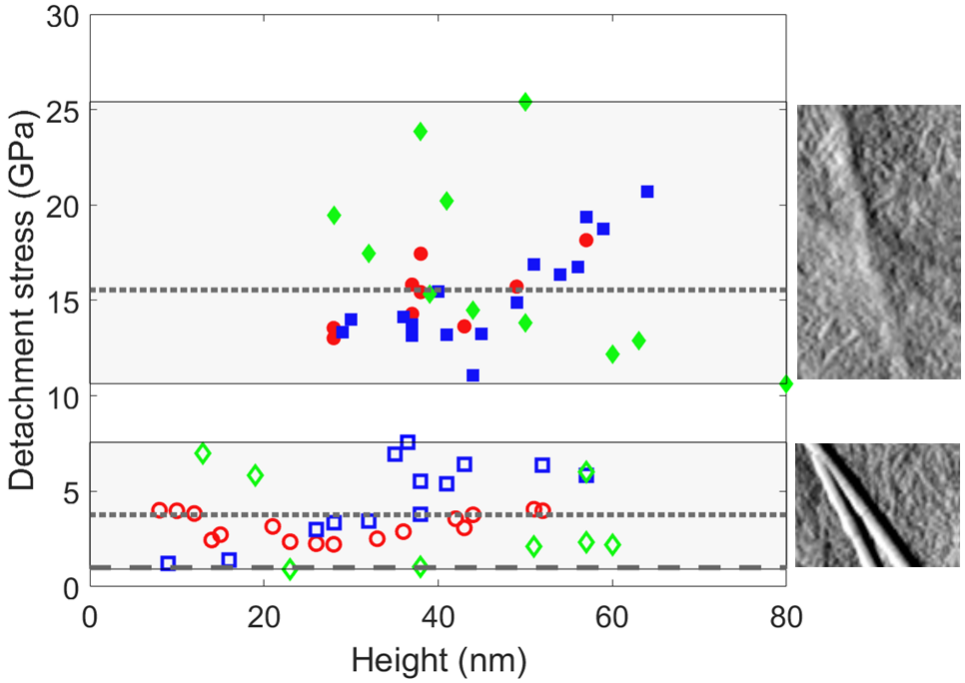

Figure 6. Detachment stress of the embedded (solid dots) and non-embedded (open dots) silver nanowires on glass (red circles), Powercoat HD paper (blue squares) and Sylvicta paper (green diamonds). A grey box including all measurements for the two nanowire morphologies is displayed. The dotted grey lines show the average value of the detachment stress in both configurations, and the dashed grey line is the yield strength of AgNWs [34,36]